

Characterization of carbon deposit with controlled carburization degree*

A. HELMINIAK[†], E. MIJOWSKA, W. ARABCZYK

West Pomeranian University of Technology, ul. Pulaskiego 10, 70-322 Szczecin, Poland

Promoted nanocrystalline iron was carburized in a differential tubular flow reactor with thermogravimetric measurement of mass changes. The carburization process was carried out in the presence of pure methane under atmospheric pressure at 650 °C to obtain different carburization degrees of the sample. The carburized iron samples were characterized by the X-ray diffraction, high-resolution transmission electron microscope in the energy-dispersive X-ray spectroscopy mode, thermoprogrammable oxidation, and Raman spectroscopy. As a result of the methane decomposition on the nanocrystalline iron the following nanocrystalline products were observed: iron carbide Fe₃C, graphite, iron and nanotubes. The crystallinity of the samples increased with the carburization degree.

Keywords: *nanocrystalline iron; carburization process; carburization degree; carbon deposit; iron carbide*

© Wrocław University of Technology.

1. Introduction

Carbon nanotubes, described for the first time by L.V. Radushkevich and V.M. Lukyanovich in 1952 [1], exhibit unique physical and chemical properties. The high specific surface and mechanical resistance, specific electrical conduction (resulting from the nanotube morphology) encourage making use of them in materials science or electronic technology. The growth of carbon nanotubes has been the subject of interest of scientists from all over the world. A lot of research has been carried out to obtain carbon nanotubes of high crystallinity. It is important to select the optimum conditions such as the temperature, pressure, catalyst or carbon source. Several techniques can be used to obtain carbon nanotubes including arc-discharge, laser ablation or chemical vapor deposition.

Catalytic decomposition of hydrocarbons is one of the promising methods for preparation of filamentous carbon forms on a bulk scale [2]. It has been proved that Fe, Co and Ni supported on SiO₂, Al₂O₃ and MgO are effective catalysts for synthesis

of filamentous carbons through hydrocarbon decomposition [2–5].

Ermakova with co-workers [6] prepared the catalysts by the heterophase sol-gel method, based on impregnation of a porous precursor of the active component, iron oxide (Fe₂O₃) with the precursor of a textural promoter taken in the estimated amount. The role of the textural promoter was to stabilize the active component structure and to prevent its sintering in the course of post treatments. Hard-to-reduce oxides (HRO) such as silica (SiO₂), alumina (Al₂O₃), titanium dioxide (TiO₂), and zirconium oxide (ZrO₂) were used as textural promoters. Both the influence of the precursors on the ability of iron to decompose methane and the influence of chemical structure of oxides on the obtained carbon structure were studied. When the iron oxide was not promoted by the above mentioned oxides it was only the temperature of the catalyst reduction that had an influence on the growth of filaments. The most promising results on elongation of the catalyst lifetime were obtained with an addition of the promoter (silica) to the iron catalyst. Different results were obtained using the pristine iron catalyst without introduction of other HROs, such as TiO₂, ZrO₂, and Al₂O₃. The TEM studies of carbon deposits demonstrated that the morphology of carbon filaments,

*This paper was presented at the Conference Functional and Nanostructured Materials, FNMA 11, 6–9 September 2011, Szczecin, Poland.

[†]E-mail: agnieszka.helminiak@wp.pl

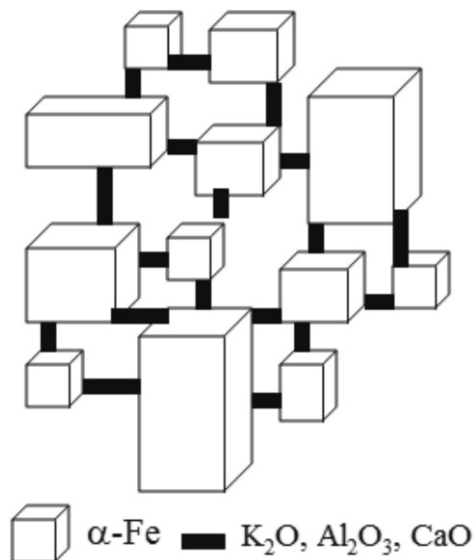


Fig. 1. The catalyst structure.

unlike the carbon yield, was strongly dependent on the chemical nature of the hard-to-reduce oxides introduced into the iron catalyst. Metal-filled carbon nanotubes were observed in the deposit obtained after 1 h of the process. Different forms of carbon were obtained after addition of hard-to-reduce oxides.

Takenaka and co-workers [2] compared the influence of the Al_2O_3 and SiO_2 catalytic supports for Fe_2O_3 used as the catalyst in methane decomposition. The efficiency of the obtained carbon deposit was higher for $\text{Fe}_2\text{O}_3/\text{Al}_2\text{O}_3$, which can be explained by the particle size of the catalytically active particles such as α -Fe and iron carbide Fe_3C . The average particle size of the catalytically active species in $\text{Fe}_2\text{O}_3/\text{Al}_2\text{O}_3$ did not change appreciably despite an increase in the loading, while the size in $\text{Fe}_2\text{O}_3/\text{SiO}_2$ became larger. Fe_2O_3 crystallites with diameters smaller than ca. 30 nm in the raw catalysts were transformed into α -Fe metal and Fe_3C (cementite) immediately after the contact with methane at 1073 K, while those with larger diameters – into γ -Fe saturated with carbon atoms (austenite). The structures of carbons formed during the methane decomposition were dependent on the catalytic support. $\text{Fe}_2\text{O}_3/\text{Al}_2\text{O}_3$ formed multi-walled and chain-like carbon nanotubes. $\text{Fe}_2\text{O}_3/\text{SiO}_2$ formed filamentous carbons and many spherical carbon particles.

The catalyst used in this work as the main component contained nanocrystalline iron (93 %) in contradistinction to the supported catalyst where the main components are HROs. In addition to iron, the catalyst contained such promoters as: aluminum oxide (Al_2O_3), calcium oxide (CaO) and potassium oxide (K_2O). Nanocrystallites of iron are connected by bridges formed by promoters. Oxides wet the iron surface and prevent the iron structure from sintering at higher temperatures, creating a mechanically stable structure [7]. The catalyst structure is shown in Fig. 1. The aim of this contribution is to characterize the carbon deposit with a controlled carburization degree, formed as a result of methane decomposition on the nanocrystalline iron. The samples were analyzed by means of X-ray diffraction (XRD), high-resolution transmission electron microscope (TEM) with energy-dispersive X-ray spectroscopy (EDX) as its mode, thermoprogrammable oxidation (TPO), and Raman spectroscopy.

2. Experimental

The method of obtaining nanocrystalline iron doped with hard-to-reduce oxides has been described in more detail elsewhere [8, 9]. The content of the promoters was estimated via the inductively coupled plasma atomic emission spectroscopy method (AES-ICP). It showed that the content was 3.3 wt.% of Al_2O_3 , 2.8 wt.% of CaO and 0.65 wt.% of K_2O . Using thermal desorption of nitrogen the specific surface area of pre-reduced nanocrystalline iron was determined to be $9 \text{ m}^2/\text{g}$. The mean size of iron nanocrystallites was determined by means of the X-ray diffraction method and rated by Sherrers equation to be 32 nm. The void ratio of the iron catalyst was $\epsilon = 0.5$.

The catalytic decomposition of methane was realized in a flow tubular reactor with thermogravimetric measurement of mass changes. The nanocrystalline iron was placed in the platinum basket in the form of a single layer of grains 1.2–1.5 mm in diameter.

The sample was reduced polythermally by hydrogen under atmospheric pressure with the rate of $15 \text{ }^\circ\text{C}/\text{min}$ in order to remove the passive layer on the iron surface. When no mass loss was observed,

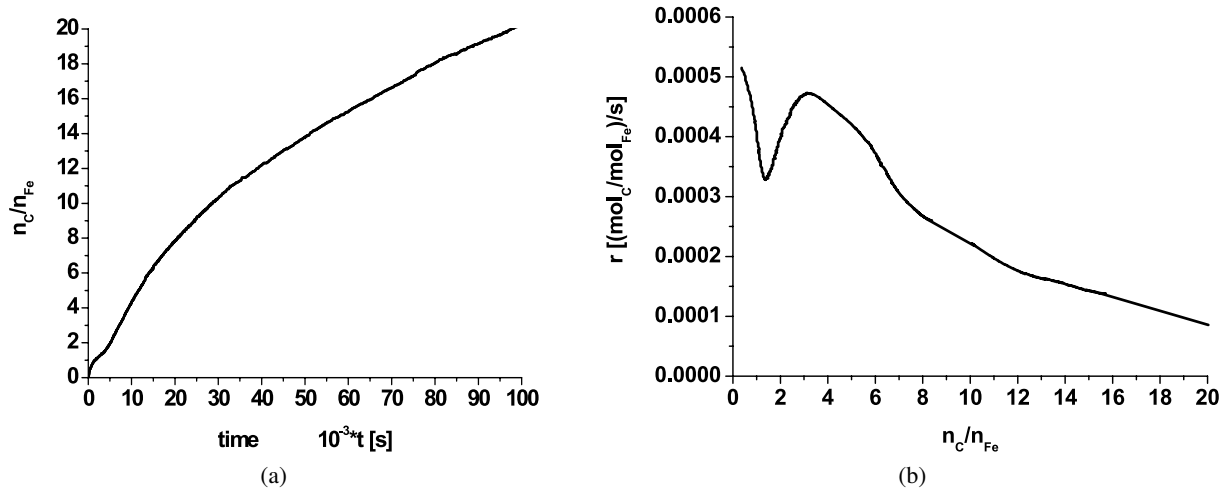


Fig. 2. a) dependence of carburization degree in time during methane decomposition on nanocrystalline iron; b) dependence of carburization rate on carburization degree of nanocrystalline iron.

nanocrystalline iron was carburized by methane at the temperature of 650 °C under atmospheric pressure to several different carburization degrees, defined as the n_C/n_{Fe} ratio of the number of carbon moles to iron moles in the carbon-iron system. The samples were cooled under methane atmosphere to room temperature.

The carburized iron samples were characterized by: XRD (XPert PRO Philips), HRTEM (FE I TECNAI G² F-20 S TWIN) with EDX, TPO (DTA-Q600, SDT TA Instruments), Raman spectroscopy (Renishaw).

Some of the carburized samples were acid treated to eliminate iron in order to determine the phase composition of carbon deposit. This step was realized via 6 M chloric acid treatment in an ultrasonication bath for 30 min. Next, the samples were subjected to multiple filtration in order to remove impurities. Subsequently, the samples were rinsed thoroughly with H₂O and acetone. Then, the samples were dried and monitored for weight-loss during the heating process in air (flow – 30 ml/min) with 5 °C/min up to 850 °C.

3. Results

The dependence of the carburization degree in time during methane decomposition on nanocrystalline iron at 650 °C is shown in Fig. 2a. The curve

is not monotonic. A characteristic curvature at the carburization degree $n_C/n_{Fe} = 1.5$ can be observed. Fig. 2b presents the dependence of the reaction rate ($r = dn_C/n_{Fe}/dt$) on the carburization degree. It indicates that after the formation of iron carbide (Fe₃C), the reaction rate decreased, reaching the minimum at $\sim n_C/n_{Fe} = 1.5$. Then, the rate increased, reaching the maximum at $\sim n_C/n_{Fe} = 3.5$. In the next stage the reaction rate decreased again.

The phase composition of the samples after carburization was determined using the X-ray method. The obtained diffraction patterns are shown in Fig. 3. The positions of peaks coming from graphite and iron are marked. The remaining reflexes come from iron carbide Fe₃C. With an increase in the carburization degree, the peaks coming from graphite and iron exhibit higher intensity, while the peaks arising from iron carbide are getting weaker. The dependence between the intensities of not overlapping peaks (C (002), Fe₃C (210), Fe (200)) as a function of carburization degrees is plotted in Fig. 4.

Two samples with carburization degrees: $n_C/n_{Fe} = 1.2$ (minimal) and $n_C/n_{Fe} = 29$ (maximal) were selected for further investigations.

The morphological studies of the samples were conducted by means of a high-resolution transmission electron microscope. Figs. 5a,b present a microscopic analysis of the samples with $n_C/n_{Fe} = 1.2$ and $n_C/n_{Fe} = 29$, respectively. The sample with

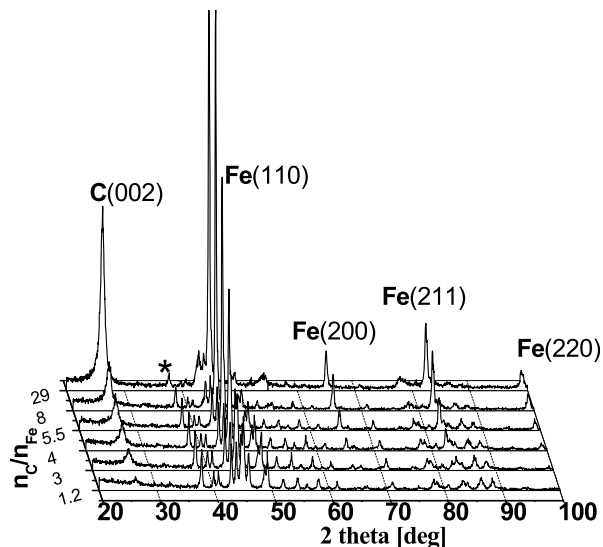


Fig. 3. Diffraction patterns of carburized samples of nanocrystalline iron. The unlabeled reflexes come from iron carbide Fe_3C phase.

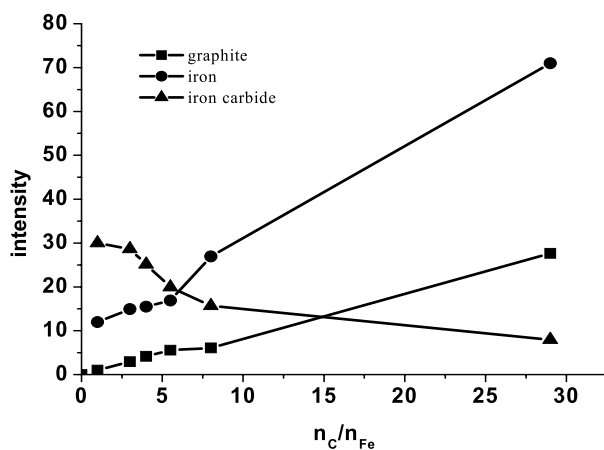


Fig. 4. Dependence of intensities of reflexes of: C (002), Fe_3C (210), Fe (200) on carburization degree of nanocrystalline iron.

lower carburization degree contains nanocrystallites of iron encapsulated in a graphitic shell with the diameter of ~ 20 nm. Aggregates composed of several carbon capsules with nanocrystallites of iron are also detected. The presence of carbon nanotubes and an amorphous structure is also observed. One can clearly see the growth of a multi-walled carbon nanotube on the iron nanocrystallite (Fig. 5a – lower panel). The nanotube grows when the nanocrystal-

lite is not fully covered by a graphitic shell. In the sample with $n_C/n_{Fe} = 29$ it can be seen that the graphitic layers (thickness ~ 25 nm) surrounding the iron nanocrystallite exhibit a much less defected structure. Carbon nanotubes and nanocapsules are detected in this sample.

The chemical composition of the samples was analyzed using energy-dispersive X-ray spectroscopy as the TEM mode. The EDX spectra of the samples are shown in the lower panels of Figs. 5a,b. The intensity of carbon peaks increases with an increase in the carburization degree of the samples. The chemical elements such as aluminum and calcium coming from promoters of the nanocrystalline iron are present. The copper signal comes from the standard TEM grid.

The Raman spectra of the samples with two carburization degrees $n_C/n_{Fe} = 1.2$ and $n_C/n_{Fe} = 29$ normalized to the G-band are shown in Fig. 6. The Raman spectra demonstrate the D and G bands. The intensity of the D-band is proportional to the concentration of defects or surface functionalization. The G/D intensity ratio is a measure of the sample purity with respect to the number of defects in the graphitic structure. The crystallinity is greater when the G/D ratio is higher. The G/D ratio for the samples $n_C/n_{Fe} = 1.2$ and $n_C/n_{Fe} = 29$ is 1.6 and 3.3, respectively. The sample exhibiting the higher carburization degree contains fewer defected graphitic structures [10, 11].

In order to establish the content of carbon fractions in the samples, the acid treated materials have been subjected to TPO studies. The thermogravimetric analysis of the samples after acid treatment showed thermal stability of the following fractions: amorphous carbon, defected graphitic structures and carbon nanotubes, which is shown in Fig. 7. The thermal stability was monitored in terms of weight-loss during the heating process in air. Fig. 7 show the approximate results of the measurements of the mass change rate for various carbon fractions, based on the calculations of the areas under the peaks in DTG (*e.g.* in Fig. 7a three main stepwise weight-losses are shown). The samples contain amorphous carbon, defected graphitic structures and carbon nanotubes. It is an approximate method and the content of carbon forms cannot be clearly defined.

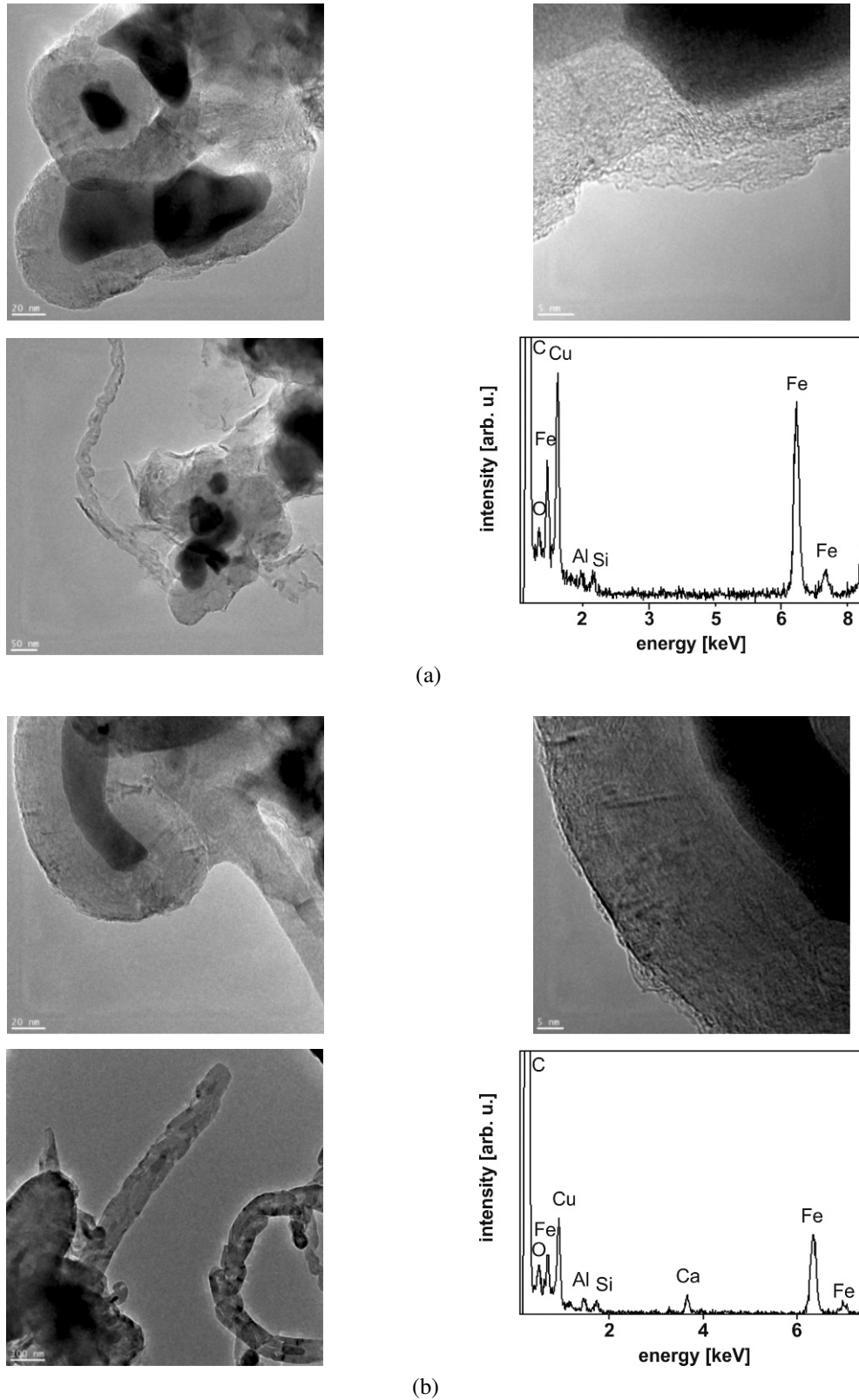


Fig. 5. TEM and EDX analysis of carburized samples of nanocrystalline iron with carburization degree: a) $n_C/n_{Fe} = 1.2$, b) $n_C/n_{Fe} = 29$.

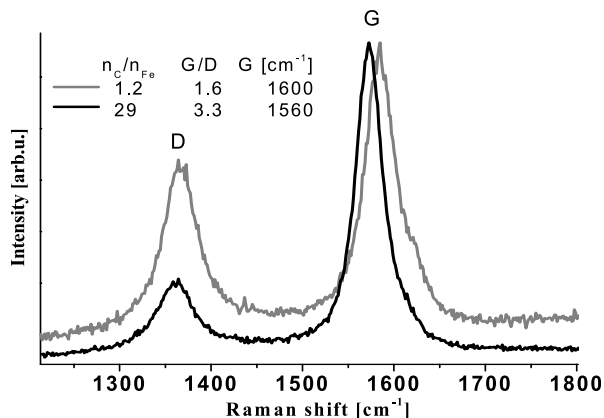


Fig. 6. Raman spectra for carburized samples of nanocrystalline iron.

4. Discussion

Due to dissociative methane adsorption on the iron surface atomic carbon dissolves in the crystalline α -Fe. With an increase in the carburization degree in the nanocrystallite, the limit of carbon absorption on α -Fe is exceeded. According to Schencks diagram [12], when nanocrystalline iron is in permanent contact with the carburization gas, the iron carbide Fe_3C and the carbon deposit is formed on the iron carbide. After coating nanocrystalline iron carbide with layers of graphite (absence of direct contact with methane) the reaction of thermal decomposition proceeds. As a result of further carburization the carbon deposit does not affect the shape of the iron crystallite.

The carbon deposit obtained during the methane decomposition on nanocrystalline iron is mostly in the form of carbon nanotubes. The sample with the higher carburization degree contains fewer defected structures. This is confirmed by the Raman and TEM analysis. The sample with the lower carburization degree is richer in defects in graphitic layers surrounding the nanocrystallite of iron. The G-band position in the Raman response of the sample with the lower carburization degree can be assigned to the weakly defected turbostratic structure of graphite. The G-band position at 1600 cm^{-1} is characteristic of materials with a low G/D ratio containing carbon nanotubes, nanofibres, amorphous carbon and defected graphitic structures. For the

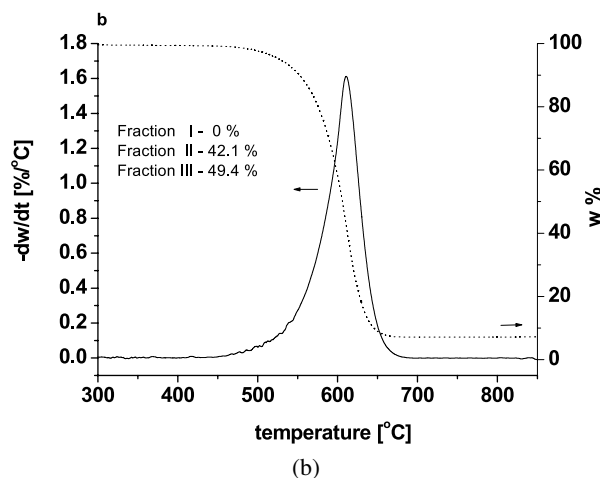
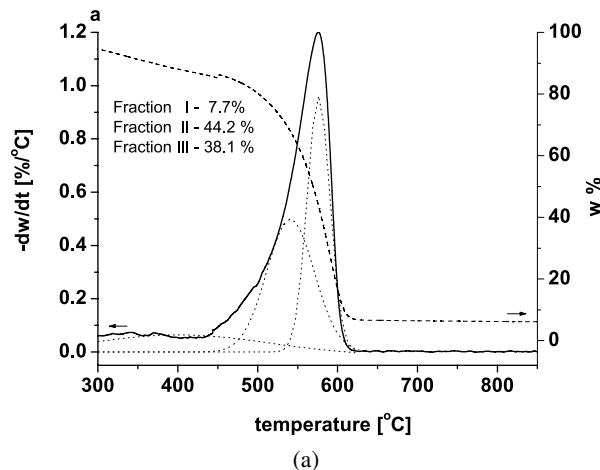


Fig. 7. TPO of acid treated nanocrystalline iron with different carburization degrees: a) $n_C/n_{Fe} = 1.2$, b) $n_C/n_{Fe} = 29$.

sample with the highest carburization degree the clusters are built of carbon atoms of sp^2 hybridization [10, 11, 13]. The thermogravimetric analysis indicates that the material with a higher carburization degree contains more carbon nanotubes than defected graphitic structures.

5. Conclusions

To summarize, methane decomposition on nanocrystalline iron promoted with aluminum, calcium and potassium oxides results in the formation of nanocrystalline iron carbide Fe_3C , nanocrystalline iron and carbon deposit in form of nanotubes, nanoshells and a tiny fraction of an amorphous struc-

ture. The carburization degree of nanocrystalline iron determines the concentration of defects in the graphitic carbon nanostructures and amorphous carbon. It was proved that the higher the carburization degree of the sample, the higher the crystallization (fewer defects) of the structures. No amorphous structure was detected in the material with the highest carburization degree. This suggests that this is a step forward to avoid amorphous carbon content in the widely studied CVD process for carbon nanotubes growth.

Acknowledgements

This research was carried out under the funding of the Polish Ministry of Science and Higher Education (NN 209 336837).

References

- [1] RADUSHKEVICH A.W., *Russ. J. Phys. Chem.*, 26, (1952) 88.
- [2] TAKENAKA S., SERIZAWA M., OTSUKA K., *J. Catal.*, 222, (2004) 520.
- [3] BAKER R.T.K., BARBER M.A., HARRIS P.S., FEATES F.S., WAITE R.J., *J. Catal.*, 26, (1972) 51.
- [4] TAKENAKA S., KOBAYASHI K., OGIHARA H., OTSUKA K., *J. Catal.*, 217, (2003) 79.
- [5] NARKIEWICZ U., PODSIADLY M., JEDRZEJEWSKI R., PELECH I., *Appl. Catal. A:General*, 384, (2010) 27.
- [6] ERMAKOVA M.A., ERMAKOV D.YU., CHUVILIN A.L., KUVSHINOV G.G., *J. Catal.*, 201, (2001) 183.
- [7] SCHLÖGL R., *Preparation and activation of the technical ammonia synthesis catalyst, Catalytic Ammonia Synthesis, Fundamentals and Practice*, J.R. Jennings, Plenum Press, New York 1991.
- [8] ARABczyk W., ZIEBRO J., KALUCKI K., SWIERKOWSKI R., JAKRZEWSKA M.J., *Chemik*, 1, (1996) 22.
- [9] ARABczyk W., KONICKI W., NARKIEWICZ U., *Solid State Phenomena*, 94, (2003) 181.
- [10] FERRARI A.C., ROBERTSON J., *Phys. Rev.*, 61, (2000) 14095.
- [11] BOROWIAK PALEN E., STEPLEWSKA A., BACHMATIUK A., RMMELI H., KALENCZUK R.K., *Mater. Sci. Forum*, 703, (2010) 636.
- [12] MELLOR J.W., *A comprehensive treatise on inorganic and theoretical chemistry*, Longman, London 1957.
- [13] SHIMODAIRA N., MASUI A., *J. Appl. Phys.*, 92, (2002) 902.

Received: 2012-09-29

Accepted: 2012-11-06